Bifunctional Lewis Acids. Synthesis and Olefin Polymerization Chemistry of the 1,1-Di[bis(perfluorophenyl)boryl]alkenes $RCH{=}C[B(C_6F_5)_2]_2$ (R = *t*-Bu, C_6H_5, C_6F_5)

Katrin Köhler,[†] Warren E. Piers,*[,†] Adam P. Jarvis,[‡] S. Xin,[‡] Y. Feng,[‡] A. M. Bravakis,[‡] Scott Collins,*[,‡] William Clegg,[§] Glenn P. A. Yap,[∥] and Todd B. Marder[⊥]

Department of Chemistry, University of Calgary, 2500 University Drive Northwest, Calgary, Alberta, Canada T2N 1N4, Department of Chemistry, University of Waterloo, Waterloo, Ontario, Canada N2L 3G1, Department of Chemistry, University of Newcastle, Newcastle upon Tyne NE1 7RU, U.K., Windsor Molecular Structure Center, Department of Chemistry and Biochemistry, University of Windsor, Windsor, Ontario, Canada N9B 3P4, and Department of Chemistry, South Road, University of Durham, Durham DH1 3LE, U.K.

Received April 6, 1998

The synthesis and characterization, including crystallographic analysis, of the bifunctional boranes $RCH{=}C[B(C_6F_5)_2]_2$ (R = *t*-C_4H_9, **1a**; C_6H_5, **1b**; C_6F_5, **1c**) by regioselective hydroboration of the corresponding 1-boraalkynes using $HB(C_6F_5)_2$ are reported herein. Compounds **1a** and **1b** have been screened as cocatalysts for ethylene polymerization in the presence of Cp_2ZrMe_2 (**3**) under a variety of conditions. NMR spectroscopic studies indicate that $Cp_2Zr[\eta^2\text{-}Bu^tC{\equiv}CB(C_6F_5)_2]$ (**4a**), $Cp_2ZrMe(C_6F_5)$, the organoborane $Me_2BC_6F_5$, and methane gas are the final products formed from reaction of **1a** with **3** in toluene solution at room temperature. The stoichiometric mechanism for this transformation has been elucidated through variable-temperature NMR studies. Complex **4a** and $MeB(C_6F_5)_2$ (**7**) were prepared independently and screened as ethylene polymerization catalysts and cocatalysts, respectively. Compound **4a** is inactive for ethylene polymerization, either alone or in the presence of additional **1a**. However, the combination of Cp_2ZrMe_2 and **7** gives rise to the species $[Cp_2ZrMe]^+[Me_2B(C_6F_5)_2]^-$ (**8**), which although unstable at room temperature in solution (decomposing over a period of 60 min to give $Cp_2ZrMe(C_6F_5)$ and the organoborane $Me_2BC_6F_5$), is active for ethylene polymerization. From a comparison of activity and MW data, it is concluded that the putative ion pairs formed from **1a** (or **1b**) and **3** lack sufficient thermal stability at conventional polymerization temperatures and that the polymerization activity observed can be interpreted as arising from species **8**.

Introduction

There has been extensive study into the development of highly active homogeneous catalytic systems for olefin polymerization over the last 15 years, with group 4 metallocene complexes figuring prominently. While, understandably, considerable attention has focused on the structure of the metallocene complex and its influence on polymerization activity and polymer properties,[1] it is now becoming increasingly evident that the nature of the cocatalyst employed in olefin polymerization can have equally dramatic effects on these features.[2]

Of the various cocatalysts used in olefin polymerization, methylaluminoxane (MAO) is the most widely employed and perhaps least well-understood.[3] There is general agreement that MAO serves as an alkylating agent (in the case of metallocene dichlorides) and also serves to ionize the metallocene dialkyl complex to form the active, cationic alkylzirconocene complex.[3b,c,4]

Conceptually related, Lewis-acidic, single-component cocatalysts have been developed and are used in combination with metallocene dialkyl complexes (either preformed or generated in situ); prototypical examples

[†] University of Calgary.
[‡] University of Waterloo.
[§] University of Newcastle.
[∥] University of Windsor.
[⊥] University of Durham.

(1) For recent reviews see (a) Kaminsky, W.; Arndt, M. *Adv. Polym. Sci.* **1997**, *127*, 144. (b) Bochmann, M. *J. Chem. Soc., Dalton Trans.* **1996**, 255. (c) Brintzinger, H. H.; Fischer, D.; Mülhaupt, R.; Rieger, B.; Waymouth, R. M. *Angew. Chem., Int. Ed. Engl.* **1995**, *34*, 1143. (c) Möhring, P. C.; Coville, N. J. *J. Organomet. Chem.* **1994**, *479*, 1.

(2) (a) Deck, P. A.; Beswick, C. L.; Marks, T. J. *J. Am. Chem. Soc.* **1998**, *120*, 1772. (b) Chen, Y.-X.; Stern, C. L.; Marks, T. J. *J. Am. Chem. Soc.* **1997**, *119*, 2582. (c) Chen, Y.-X.; Stern, C. L.; Yang, S.; Marks, T. J. *J. Am. Chem. Soc.* **1996**, *118*, 12451. (d) Giardello, M. A.; Eisen, M. S.; Stern, C. L.; Marks, T. J. *J. Am. Chem. Soc.* **1995**, *117*, 12114. (e) Hlatky, G. G.; Eckman, R. R.; Turner, H. W. *Organometallics* **1992**, *11*, 1413. (f) Yang, X.; Stern, C. L.; Marks, T. J. *Organometallics* **1991**, *10*, 840. (g) Hlatky, G. G.; Turner, H. W.; Eckman, R. R. *J. Am. Chem. Soc.* **1989**, *111*, 2728.

(3) (a) For a recent review see: Reddy, S. S.; Sivaram, S. *Prog. Polym. Sci.* **1995**, *20*, 309. See also: (b) Harlan, C. J.; Bott, S. G.; Barron, A. R. *J. Am. Chem. Soc.* **1995**, *117*, 6465. (c) Harlan, C. J.; Mason, M. R.; Barron, A. R. *Organometallics* **1994**, *13*, 2957. (d) Pasynkiewicz, S. *Polyhedron* **1990**, *9*, 429.

(4) (a) Sishta, C.; Hathorn, R. M.; Marks, T. J. *J. Am. Chem. Soc.* **1992**, *114*, 1112. (b) Gassman, P. G.; Callstrom, M. R. *J. Am. Chem. Soc.* **1987**, *109*, 7875.

S0276-7333(98)00259-3 CCC: $15.00
Publication on Web 07/15/1998

include $[Ph_3C]^+[B(C_6F_5)_4]^-$ [5] and $B(C_6F_5)_3$.[6,7] It is widely accepted that the role of these cocatalysts is to generate the highly active, coordinatively unsaturated, 14-electron species $[Cp_2MR]^+$ through alkide abstraction. However, it is clear that even noncoordinating counterions[8] can still interact with the metal center in a manner which modulates polymerization activity and possibly the rates of chain transfer in olefin polymerization.

Marks and co-workers have studied the relationship between cation−anion ion-pairing and catalytic activity in zirconocene complexes activated by $B(C_6F_5)_3$.[6] In these cases, the strength of the $Cp_2Zr^+Me(\mu\text{-}Me)B^-(C_6F_5)_3$ interaction, as revealed through X-ray diffraction studies of these ion pairs, has a decisive influence on polymerization activity and polymer molecular weight (MW). Even less-coordinating counterions such as $[B(C_6F_5)_4]$ can still interact with the metal center through formation of a Zr−F bridge, thus affecting catalytic activity and stability.[9]

Thus, the search for even less-coordinating counterions seems worthwhile from the point of view of tuning polymerization activity, catalyst stability, and other properties. In this connection, Marks and co-workers reported a number of years ago that the borohydride anion $[Bu^tCH_2CH\{B(C_6F_5)_2\}_2(\mu\text{-}H)]$ as its tributylammonium salt was an active cocatalyst for ethylene polymerization.[10] Despite this report, much less attention has been given to bis-boryl compounds incorporating $B(C_6F_5)_2$ units (**I**) which, by analogy to $B(C_6F_5)_3$, might also be useful cocatalysts for ethylene polymerization.[11] In the resulting counteranion, the negative

I

charge is potentially delocalized over more atoms, reducing the Coulombic interactions between the cation and anion in a catalytically active ion pair and giving a more electron-deficient, more reactive cation. Variation in the nature of the backbone linking the two Lewis-acid centers offers the opportunity to tune the chelating properties of the activator as well as the extent of delocalization of charge.

Scheme 1

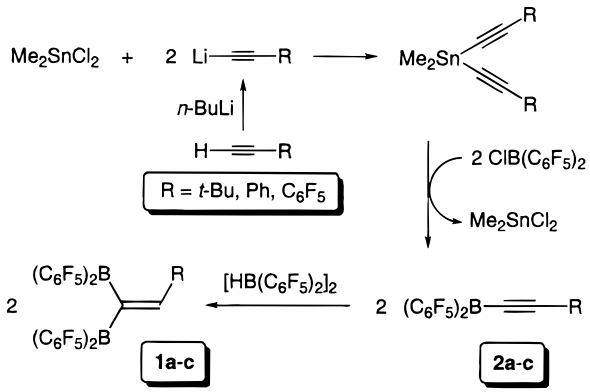

Hydroboration of terminal alkynes with the highly electrophilic borane $HB(C_6F_5)_2$ offers a convenient route to a variety of fully saturated bidentate boranes[12] with a one-carbon linker, i.e., $RCH_2CH[B(C_6F_5)_2]_2$. Unfortunately, these compounds tend to undergo facile retrohydroboration and their reaction chemistry can be dominated by the small amounts of $HB(C_6F_5)_2$ present as a result.[13] To be effective cocatalysts for olefin polymerization, their conversion to a hydridoborate anion is necessary;[10] an alternative approach would be to eliminate the possibility of retrohydroboration. Herein, we describe the synthesis and characterization of the unsaturated diboranes $RCH{=}C[B(C_6F_5)_2]_2$ (R = *t*-C_4H_9, **1a**; C_6H_5, **1b**; C_6F_5, **1c**) which do not undergo β-elimination. Their reactions with Cp_2ZrMe_2 and efficacy as catalyst activators are also discussed.

Results and Discussion

The diboranes **1** were synthesized by the common route shown in Scheme 1. Bis(alkynyl)dimethyltin compounds were prepared from in situ generated lithium acetylide and dimethyltin dichloride and purified prior to use in a transmetalation reaction with $ClB(C_6F_5)_2$. These reactions, carried out at −78 °C, yielded the alkynyl boranes **2**, which could be isolated (**2a**, 85%;[14] **2b**, 75%) or used in situ in the next step of the sequence. As pure solids, the alkynyl boranes are stable for several weeks if stored at −35 °C but decompose slowly (days) in solution. Many alkynyl boranes with less electron-withdrawing substituents have been prepared,[15] but

(5) (a) Bochmann, M.; Lancaster, S. J. *Organometallics* **1993**, *12*, 633. (b) Bochmann, M.; Lancaster, S. J. *J. Organomet. Chem.* **1992**, *434*, C1. (c) Chien, J. C. W.; Tsai, W.-M.; Rausch, M. D *J. Am. Chem. Soc.* **1991**, *113*, 8570. (d) Turner, H. W. Eur. Pat. Appl. EP 0277004, 1988.

(6) (a) Yang, X.; Stern, C. L.; Marks, T. J. *J. Am. Chem. Soc.* **1994**, *116*, 10015. (b) Yang, X.; Stern, C. L.; Marks, T. J. *J. Am. Chem. Soc.* **1991**, *113*, 3623. For work on related boranes, see ref 2c.

(7) Piers, W. E.; Chivers, T. *Chem. Soc. Rev.* **1997**, 345.

(8) For a review, see: Strauss, S. H. *Chem. Rev.* **1993**, *93*, 927.

(9) (a) Jia, L.; Yang, X.; Stern, C. L.; Marks, T. J. *Organometallics* **1997**, *16*, 842. (b) Temme, B.; Erker, G.; Karl, J.; Luftmann, H.; Fröhlich, R.; Kotila, S. *Angew. Chem., Int. Ed. Engl.* **1995**, *34*, 1755. We have also noted binding of $[B(C_6F_5)_4]^-$ to cationic methylzirconocene complexes, even in polar solvents (e.g., toluene:chlorobenzene mixtures) at low temperatures (i.e., Zr−Me signals coupled to F), although solvent-separated, ion-pairs predominate under these conditions. Xin, S.; Collins, S. manuscript in preparation.

(10) (a) Jia, L.; Yang, X.; Stern, C.; Marks, T. J. *Organometallics* **1994**, *13*, 3755. (b) Marks, T. J.; Jia, L.; Yang, X. U.S. Patent 5,447,895, 1995 (Northwestern University). (c) Galsworthy, J. R.; Green, M. L. H.; Williams, V. C.; Chernega, A. N. *Polyhedron* **1998**, *17*, 119.

(11) Marks and co-workers have also noted that the organodiborane, $Bu^tCH_2CH[B(C_6F_5)_2]_2$, was an effective cocatalyst for ethylene polymerization but indicated that this material was unstable with respect to formation of $B(C_6F_5)_3$.[9a]

(12) Parks, D. J.; Spence, R. E. v H.; Piers, W. E. *Angew. Chem., Int. Ed. Engl.* **1995**, *34*, 809.

(13) For example, $HB(C_6F_5)_2$ is highly reactive toward neutral bis(alkyl)zirconocenes, see: (a) Spence, R. E. v H.; Parks, D. J.; Piers, W. E.; MacDonald, M.; Zaworotko, M. J.; Rettig, S. J. *Angew. Chem., Int. Ed. Engl.* **1995**, *34*, 1230. (b) Sun, Y.; Piers, W. E.; Rettig, S. J. *Organometallics* **1996**, *15*, 4110. (c) Sun, Y.; Spence R. E. v H.; Piers, W. E.; Parvez, M.; Yap, G. P. A. *J. Am. Chem. Soc.* **1997**, *119*, 5132. (d) Piers, W. E. *Chem. Eur. J.* **1998**, *4*, 13.

(14) An X-ray structural analysis of **2a** established the connectivity and general features of the compound's structure; however, severe disorder precluded adequate refinement of the details associated with the structure.

(15) For examples, see: (a) Wrackmeyer, B.; Nöth, H. *Chem. Ber.* **1977**, *110*, 1086. (b) Wrackmeyer, B. *Z. Naturforsch.* **1982**, *37b*, 788. (c) Maderna, A.; Pritzkow, H.; Siebert, W. *Angew. Chem., Int. Ed. Engl.* **1996**, *35*, 1501. (d) Schulz, H.; Gabbert, G.; Pritzkow, H.; Siebert, W. *Chem. Ber.* **1993**, *126*, 1593. (e) Curtis, M. A.; Müller, T.; Beez, V.; Pritzkow, H.; Siebert, W.; Grimes, R. N. *Inorg. Chem.* **1997**, *36*, 3602. (f) Wrackmeyer, B.; Schanz, H.-J.; Milius, W. *Angew. Chem.* **1997**, *109*, 1145. (g) Meller, A.; Maringgele, W.; Elter, G.; Bromm, D.; Noltemeyer, M.; Sheldrick, G. M. *Chem. Ber.* **1987**, *120*, 1437. (h) Köster, R.; Boese, R.; Wrackmeyer, B.; Schanz, H.-J. *J. Chem. Soc., Chem. Commun.* **1995**, 1691.

those with more electrophilic boron centers tend not to be isolable.[16] Indeed, compound **2c** was less stable than the other two derivatives and was best used in situ for the next step of the synthesis.

Hydroboration of compounds **2** with 1 equiv of $HB(C_6F_5)_2$ yielded the 1,1-alkenyl diboranes **1** in good to excellent yields. On electronic grounds, this hydroboration was predicted to give the geminal-substituted products **1** as shown; indeed, the reactions proceed with >95% regioselectivity. The diboranes **1** were initially formulated as the 1,1-substituted alkenyl derivatives on the basis of their NMR spectra; this was subsequently confirmed crystallographically (vide infra). Resonances for the =CH moiety in both the ^1H and ^{13}C NMR spectra are shifted downfield from values typical of olefinic carbons and hydrogens due to the electron-withdrawing $B(C_6F_5)_2$ groups. For **1a**, these signals appear at 7.16 and 183.6 ppm, respectively. Both signals are slightly broadened by the quadrupolar boron nuclei, an effect which precluded detection of the olefinic carbon directly attached to the boron atoms. The most convincing evidence for geminal substitution came in the form of NOE experiments on **1a**, which exhibited strong enhancements between the olefinic proton and the *tert*-butyl group. Such observations would not be expected if these groups were trans disposed about the carbon−carbon double bond in a 1,2-substituted product.

Quadrupolar broadening also had a significant impact on the ^{11}B NMR data; spectra for each diborane **1** were extremely broad, and the inequivalent boron nuclei could not be distinguished at the field employed. Although no fine structure was observed in these resonances, scalar coupling between the chemically inequivalent boron nuclei also likely contributes to the broadness of the signals. The resonances observed for **1a** (39.9 ± 1.0), **1b** (62.7 ± 1.0), and **1c** (61.8 ± 1.0) are all, however, in the region expected for neutral, three-coordinate boranes.[17] Fluorine-19 NMR spectroscopic data is more useful in distinguishing the two different $-B(C_6F_5)_2$ moieties in that two sets of *ortho*, *para*, and *meta* resonances are observed for each compound at room temperature. For **1c**, a third set of resonances for the olefinic C_6F_5 group is also observed.

X-ray Structures of 1a−c. The 1,1-diboryl substitution pattern for each of the diboranes **1a−c** was confirmed via X-ray crystallography; the molecular structures are shown in Figures 1−3, while selected metrical parameters are given in Table 1. Note that the numbering scheme for **1a** is slightly different than that for **1b** and **1c**; Table 1 is constructed so that each entry refers to the same parameter for each structure.

In all three structures, the boron center trans to the R substituent lies essentially in conjugation with the C=C bond, i.e., the boron trigonal plane is roughly coincident with the olefin plane. This is approximated by the first pair of torsion angles listed in Table 1. For phenyl-substituted **1b**, these parameters suggest that the B_{trans} trigonal plane is rotated ca. 4° out of coplanarity with the olefin plane while for **1a** and **1c** with their bulkier substitutions the deviation from coplanarity is more severe at ca. 15−19°. Nonetheless, the trans $-B(C_6F_5)_2$ moiety's effect on the C(1)−C(2) lengths in these compounds is apparent in that each exhibits C=C bonds elongated by 0.02−0.03 Å over the typical C=C distance of 1.335 Å.[18] The longest C=C bond is observed in **1b**, where conjugation is most pronounced. Conversely, the cis boron centers are rotated out of conjugation with C=C (see the second pair of torsion angles listed) to avoid severe steric interactions with the olefinic R group. Another measure of the steric crowding in these compounds is the ca. 10−12° of twisting about the C=C double bonds seen in each compound, as illustrated by the third pair of torsion angles given.

The congestion about the C=C double bond is also manifested by the angles about C(1) and C(2) which stray from ideal values of 120°. This is particularly true for **1a**, in which the C(2)−C(1)−B_{cis} and C(2)−C(1)−

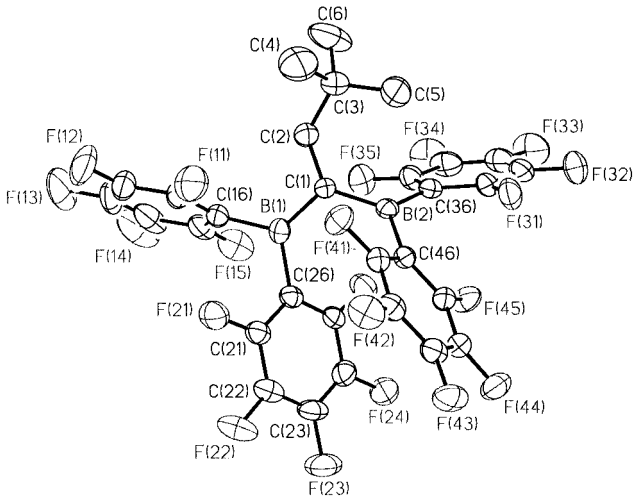

Figure 1. ORTEP diagram of **1a** (thermal ellipsoids are at the 50% probability level).

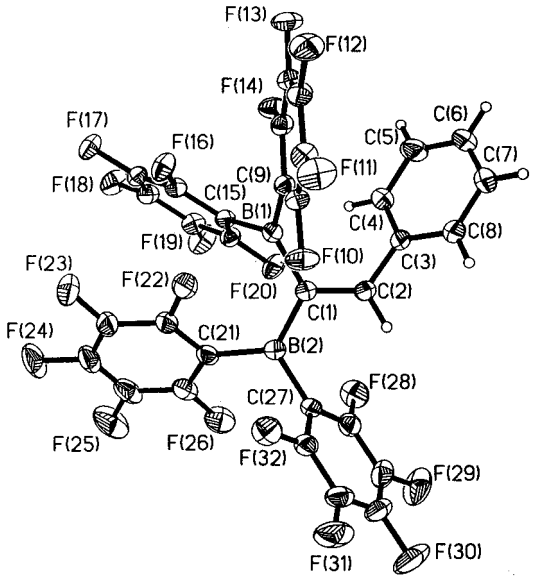

Figure 2. ORTEP diagram of **1b** (thermal ellipsoids are at the 50% probability level). Unlabeled carbon atoms have the same number as the corresponding F atom.

(16) Leung, S.-W.; Singleton, D. A. *J. Org. Chem.* **1997**, *62*, 1955 and references therein.

(17) Kidd, R. G. In *NMR of Newly Accessible Nuclei*; Laszlo, P., Ed.; Academic Press: New York, 1983; Vol. 2.

(18) Gordon, A. J.; Ford, R. A. *The Chemist's Companion*; Wiley and Sons: New York, 1972; p 108.

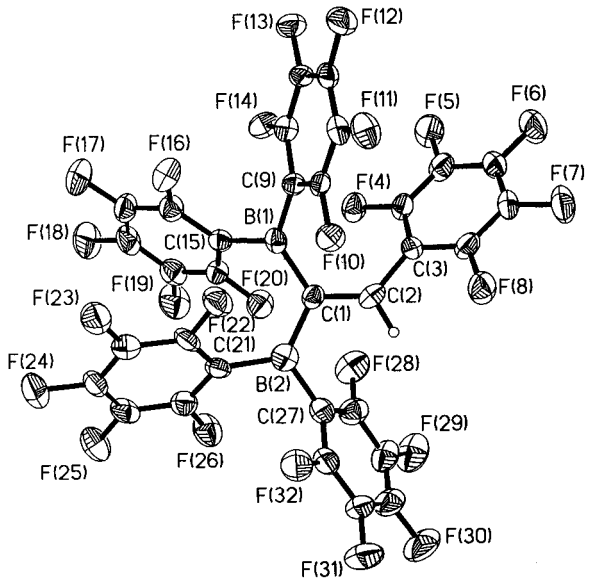

Figure 3. ORTEP diagram of **1c** (thermal ellipsoids are at the 50% probability level). Unlabeled carbon atoms have the same number as the corresponding F atom.

B_{trans} angles are 125.8(5)° and 115.4(5)°, respectively, and C(1)−C(2)−C(3) is 131.4(5)°. In the aryl-substituted derivatives **1b**−**c**, the interactions between R and $B_{cis}(C_6F_5)_2$ are less severe because of the aryl groups' ability to rotate out of conjugation with the C=C double bond by 34.4° and 40.3°, respectively (Table 1). In these two compounds, the B_{cis}−C(1)−B_{trans} angles are larger than that found in **1a** while the C(2)−C(1)−B angles are closer to normal values.

The steric tensions in these molecules, coupled with the fact that the two boron trigonal planes approach orthogonality, have some implications for how the boron centers might (or might not) act in concert as Lewis acids. Although the cis boron center might be expected to be more Lewis acidic since it is not in conjugation with C=C, both faces of the trigonal plane are sterically blocked, one by the cis R substituent and the other by a C_6F_5 group on the other $B(C_6F_5)_2$ moiety. Indeed, the region of space between the boron centers in these molecules is quite crowded and, at least by appearances, inaccessible to Lewis bases. Consequently, **1a** does not appear to coordinate THF even in solution and the binding of simple ketones such as acetone is reversible.[19] The open face of the conjugated $B_{trans}(C_6F_5)_2$ group thus appears, a priori, to be the most likely site of reactivity for these molecules. This prediction is born out in the reactions of **1a** with dimethylzirconocene, which are described in detail below.

Reactions of 1a with Cp_2ZrMe_2. Since the 1,1-alkenyl boranes serve as effective activators in olefin polymerization experiments (vide infra), the reactions of **1a** with dimethylzirconocene were examined in detail.[20] When reacted in a 1:1 ratio, the product mixture included one-half of the starting borane, suggesting that a 2:1 ratio of [Zr]:**1a** would be more appropriate. This was born out as depicted in Scheme 2; when the reagents are mixed in this ratio at −78 °C and allowed to react under gradually warming conditions, clean formation of the product mixture shown is observed.

Methane was identified by its characteristic proton chemical shift in C_6D_6 of 0.16 ppm, while ^1H, ^{11}B, and ^{19}F NMR data clearly indicate the presence of dimethylpentafluorophenylborane (see Experimental Section). Of the two zirconium-containing products, $Cp_2Zr(C_6F_5)CH_3$ is implicated by the characteristic triplet at 0.32 ppm ($^5J_{HF}$ = 3.9 Hz) for the methyl group along with ^{19}F NMR data consistent with the presence of a Zr−C_6F_5 moiety. Similar data was observed for a related derivative, $[1,3\text{-}(SiMe_3)_2C_5H_3]_2Zr(C_6F_5)CH_3$, reported by Marks et al.[6a] The other organometallic species present in the same molar ratio as $Cp_2Zr(C_6F_5)CH_3$ we formulate as the intriguing zirconocene alkyne complex $Cp_2Zr[\eta^2\text{-}Bu^tC{\equiv}CB(C_6F_5)_2]$, **4a**. Although the intimate structural details of this compound have yet to be determined, the spectroscopic and analytical data obtained are consistent with the gross features depicted. Furthermore, this compound could be synthesized separately and isolated analytically pure by reaction of the boryl acetylide **2a** with $[Cp_2Zr(H)CH_3]_n$ as shown in Scheme 3. This reaction is accompanied by methane evolution, which likely occurs from a boravinyl methyl zirconocene[21] formed by regioselective hydrozirconation of **2a**; this intermediate was not observed.

The reaction of Cp_2ZrMe_2 with **1a** (in a 2:1 ratio) was carried out at low temperature in an NMR tube and monitored by both ^1H and ^{19}F NMR spectroscopy. The results of these experiments are consistent with the chemistry shown in Scheme 4. At − 60 °C, a rapid reaction between the two reactants occurs, forming the product **5a**, which is stable for several hours under these conditions. This ion pair, containing a binuclear cation, is very similar to that formed from various dimethyl zirconocenes and the sterically bulky fluoroborane tris(2,2′,2″-perfluorobiphenyl)borane as reported by Marks et al.[2c,22] The dimeric cation is implicated by the observed stoichiometry of the reaction along with signals in the ^1H NMR spectrum at −0.10 and −1.23 ppm (found in a 2:1 ratio) which are characteristic of the terminal and bridging methyl groups.[22] Dinuclear cations such as this form when the counterion is a poorer base than dimethylzirconocene itself and attest to **1a**'s ability to form a very weakly coordinating counterion.

This ability is not, however, due to chelation of the abstracted methide. Proton spectroscopic data associated with the counteranion suggest that the diborane utilizes only one of the boron centers to abstract the alkyl group. In the ^1H NMR spectrum at −60 °C, the resonance for the BCH_3 group appears at −0.39 ppm as a broad signal; NOE experiments in which this signal is irradiated show strong enhancement in the resonance due to the vinylic proton at 6.31 ppm, while a negligible effect on the resonance for the *tert*-butyl protons was observed. A reciprocal enhancement in BCH_3 was found when the irradiation was directed to the 6.31 ppm resonance. Together, these results imply that the borate methyl group is cis to the olefinic proton; a

(19) Köhler, K.; Piers, W. E. *Can. J. Chem.*, submitted for publication.

(20) Reactions of Cp_2ZrMe_2 and **1b** had essentially the same outcome but were not studied in as much detail.

(21) (a) Buchwald, S. L.; Watson, B. T.; Huffman, J. C. *J. Am. Chem. Soc.* **1987**, *109*, 2544. (b) Neilsen, R. B.; Buchwald, S. L. *Chem. Rev.* **1988**, *88*, 1047.

(22) Chen, Y.-X.; Marks, T. J. *Organometallics* **1997**, *16*, 3649.

Table 1. Selected Metrical Parameters for Diboranes 1a−c

	1a		1b	1c
		Bond Distances (Å)		
C(1)−C(2)	1.357(7)	C(1)−C(2)	1.365(2)	1.357(6)
C(2)−C(3)	1.504(8)	C(2)−C(3)	1.454(2)	1.456(6)
B(1)−C(1)	1.544(8)	B(2)−C(1)	1.540(2)	1.555(7)
B(2)−C(1)	1.564(8)	B(1)−C(1)	1.564(2)	1.561(6)
B(1)−C(16)	1.601(7)	B(2)−C(27)	1.591(2)	1.580(7)
B(1)−C(26)	1.613(7)	B(2)−C(21)	1.578(2)	1.566(7)
B(2)−C(36)	1.622(7)	B(1)−C(9)	1.585(2)	1.569(6)
B(2)−C(46)	1.618(6)	B(1)−C(15)	1.577(2)	1.586(6)
		Bond Angles (deg)		
C(2)−C(1)−B(1)	115.4(5)	C(2)−C(1)−B(2)	117.48(13)	115.7(4)
C(2)−C(1)−B(2)	125.8(5)	C(2)−C(1)−B(1)	119.24(13)	122.5(4)
B(1)−C(1)−B(2)	118.7(4)	B(1)−C(1)−B(2)	123.22(13)	121.7(4)
C(1)−C(2)−C(3)	131.4(5)	C(1)−C(2)−C(3)	124.04(13)	129.9(4)
C(1)−B(1)−C(16)	124.2(5)	C(1)−B(2)−C(27)	120.55(13)	120.0(4)
C(1)−B(1)−C(26)	122.8(4)	C(1)−B(2)−C(21)	122.04(13)	121.9(4)
C(16)−B(1)−C(26)	112.9(4)	C(21)−B(2)−C(27)	117.40(13)	118.2(4)
C(1)−B(2)−C(36)	119.9(4)	C(1)−B(1)−C(15)	122.53(12)	118.4(4)
C(1)−B(2)−C(46)	118.6(4)	C(1)−B(1)−C(9)	119.36(12)	121.7(4)
C(36)−B(2)−C(46)	121.0(4)	C(15)−B(1)−C(9)	117.94(12)	119.9(4)
		Torsion Angles (deg)		
C(16)−B(1)−C(1)−C(2)	12.3(8)	C(27)−B(2)−C(1)−C(2)	4.5(2)	−17.8(6)
C(26)−B(1)−C(1)−C(2)	−165.8(5)	C(21)−B(2)−C(1)−C(2)	−176.1(2)	161.4(4)
C(36)−B(2)−C(1)−C(2)	−72.1(7)	C(15)−B(1)−C(1)−C(2)	131.6(2)	143.5(4)
C(46)−B(2)−C(1)−C(2)	115.7(6)	C(9)−B(1)−C(1)−C(2)	−53.1(2)	−36.6(6)
B(1)−C(1)−C(2)−C(3)	164.5(6)	B(2)−C(1)−C(2)−C(3)	169.7(2)	169.3(4)
B(2)−C(1)−C(2)−C(3)	−10.3(9)	B(1)−C(1)−C(2)−C(3)	−12.9(2)	−10.6(7)
		C(1)−C(2)−C(3)−C(4)	−34.4(2)	−40.2(7)

Scheme 2

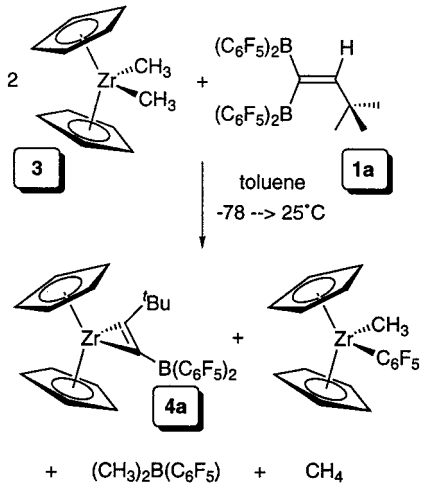

Scheme 3

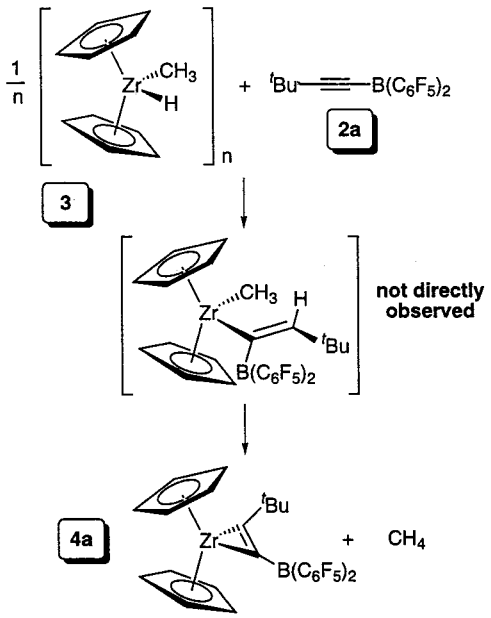

chelated methide anion would not be expected to exhibit NOE enhancements to either of the olefinic groups. In the ^{19}F NMR spectrum at −60 °C, 20 different resonances are observed, indicating that all four C_6F_5 groups are chemically distinct and that rotation of each of the aryl rings is restricted. Complete assignment of this spectrum and conclusions as to the coordination environments about the boron centers based on the relative chemical shifts[23] of the *meta* and *para* fluorine resonances were not possible.

Upon warming to −40 °C, **5a** undergoes decomposition to various products, a process which begins with the loss of $CH_3B(C_6F_5)_2$ from the anion. The resulting vinyl anion, which is likely stabilized to some extent by the strongly electron-withdrawing $-B(C_6F_5)_2$ group,[24] reacts with the zirconocene cation to form the boravinyl methyl zirconocene precursor to **4a**. Again, this species is not observed, not surprising given its propensity to lose methane. The other products of the decomposition of ion pair **5a**, i.e., Cp_2ZrMe_2 and $CH_3B(C_6F_5)_2$, are also not spectroscopically observed in this process; rather, they react together rapidly under these conditions to give a different ion pair $[Cp_2ZrMe]^+[Me_2B(C_6F_5)_2]^-$, **8**, as shown in Scheme 4. This can be shown to occur in a separate experiment using Cp_2ZrMe_2 and $CH_3B(C_6F_5)_2$. This latter experiment also reveals the tendency of ion pair **8** to decompose at higher temperatures to the neutral products $Cp_2ZrMeC_6F_5$ and $Me_2BC_6F_5$, which

(23) Horton, A. D.; de With, J. *Organometallics* **1997**, *16*, 5424.

(24) Krishnamurthy, S.; Brown, H. C. *J. Org. Chem.* **1980**, *45*, 849. (b) Yoshida, T.; Negishi, E. *J. Chem. Soc., Chem. Commun.* **1974**, 763. (c) Pelter, A.; Smith, K.; Brown, H. C. *Borane Reagents*; Academic Press: New York, 1988; p 22−23.

Scheme 4

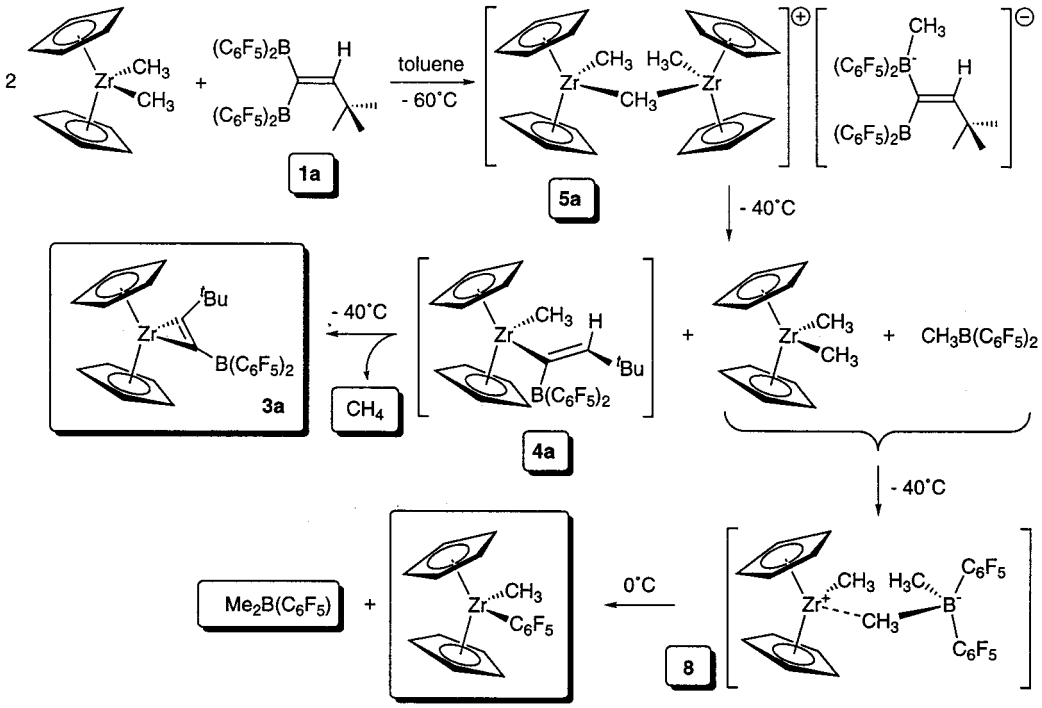

Scheme 5

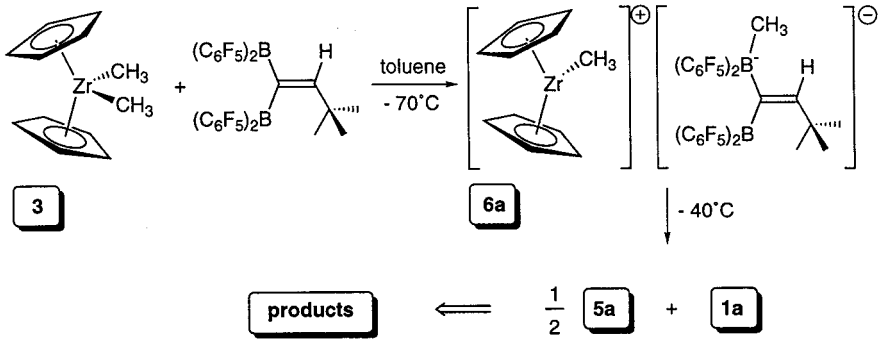

occurs with a half-life of about 20 min at room temperature. This accounts for the presence of these neutral compounds in the product mixture of the reaction between **1a** and dimethylzirconocene.

A final observation concerning this system involves the course of the reaction when dimethyl zirconocene and **1a** are mixed in a 1:1 ratio at −60 °C (Scheme 5). This reaction shows that dinuclear cation formation is not favored over further methyl abstraction, as was the case when the bulkier tris(2,2′,2″-perfluorobiphenyl)-borane was employed.[2c,22] The ion pair **6a** was characterized by ^{1}H NMR spectroscopy and underwent conversion to dinuclear **5a** and **1a** at temperatures where decomposition of **5a** ensued, precluding quantitative measurements of the equilibrium between these two species. The final product mixture of this reaction was the same as that in the 2:1 reaction with the addition of 0.5 equiv of diborane **1a**.

Ethylene Polymerizations with Boron Cocatalysts. Ethylene polymerizations using **1a**, **1b**, and, for comparison purposes, $B(C_6F_5)_3$ as cocatalysts with Cp_2ZrMe_2 (**3**) were conducted in a toluene slurry under a variety of conditions, and the results are summarized in Tables 2 and 3. Two different procedures were employed, and these were found to have a considerable influence on polymerization activity and, therefore, will be discussed in sequence.

Table 2. Polymerization of Ethylene Using Cp_2ZrMe_2 (3) and Boron Cocatalysts[a]

entry	[**3**] (μM)	cocatalyst[b]	T (°C)	A (10^3 kg of PE/(mol of Zr × h))[c]
1	70.0	$B(C_6F_5)_3$	50	3.9
2	65.0	$B(C_6F_5)_3$	50	5.2
3	65.0	$B(C_6F_5)_3$	30	9.5
4	70.0	**1a**	70	3.0
5	70.0	**1a**	50	4.9
6	70.0	**1a**	50	5.5
7	70.0	**1b**	70	3.4
8	65.0	**1b**	50	2.0
9	65.0	**1b**	50	6.0

[a] Polymerization conditions: toluene 500 mL, 75 psig of ethylene, 1000 rpm with **3** and cocatalyst premixed in toluene solution at room temperature. [b] For each cocatalyst, 1.2 equiv with respect to **3** was employed. [c] Activity in 10^6 g PE/(mol of Zr × h), based on an impurity level of 50 μM.

The first procedure involved pre-contacting complex **3** with the appropriate cocatalyst (1.2 equiv) in a small volume of toluene at room temperature for a period of 10−15 min,[25] followed by introduction into the reactor, presaturated with monomer at the desired pressure and

Table 3. Ethylene Polymerization Using Cp_2ZrMe_2 (3) and Boron Cocatalysts[a]

entry	cocatalyst[b]	T (°C)	A[c]	M_n (K)	M_w/M_n
1	$B(C_6F_5)_3$	30	5.2 (0.5)[d]	195 (5)[d]	3.9 (0.4)[d]
2[e]	$B(C_6F_5)_3$	30	5.0 (0.5)[f]	170 (3)[f]	4.3 (0.5)[f]
3[g]	$B(C_6F_5)_3$	30	5.9 (0.4)[f]	155 (15)[f]	3.5 (0.2)[f]
4	**1a**	30	3.3 (0.3)[d]	270 (25)[d]	1.9 (0.1)[d]
5	**1a**	65	3.0 (0.3)[f]	132 (14)[f]	2.6 (0.2)[f]
6	**1b**	30	3.2 (0.2)[f]	204 (10)[f]	1.9 (0.1)[f]
7	**1b**	65	4.6 (0.3)[f]	100 (3)[f]	3.1 (0.1)[f]
8[e]	**1b**	65	1.4	108	3.43
9	**7**	30	2.4 (0.2)[d]	245 (15)[d]	2.1 (0.1)[d]

[a] Polymerization conditions: toluene 500 mL; 75 psig of C_2, 1000 rpm, 20−30 min polymerization time. [TMA] = 30 μM; Cp_2ZrMe_2 (15 μM) was injected into a saturated solution of the cocatalyst and TMA, except where noted. [b] The amount of cocatalyst present was 1.2 equiv with respect to **3**. [c] Activity in 10^6 g of PE/(mol of Zr × h). [d] Average value with estimated standard deviation in parentheses (4−6 trials). [e] Catalyst and cocatalyst were premixed prior to introduction into the reactor containing TMA. [f] Average of two trials with range in parentheses. [g] Cocatalyst (15 μM) added to a solution of Cp_2ZrMe_2 (60 μM) and monomer without TMA present.

temperature (Table 2). No scrubbing agent was employed, and as a result, quite high catalyst loadings (65−70 μM) were required to observe measurable consumption of monomer. Control experiments (at lower catalyst loadings) revealed that the level of protic impurities in the solvent/monomer system under these conditions was between 40 and 60 μM, based on [$Cp_2ZrMe(\mu$-Me)B-$(C_6F_5)_3$] (i.e., ca. 100−120 μM based on potentially reactive M−Me bonds). The activity data in Table 2 are quoted on the basis of an impurity level of 50 μM, based on similar work conducted in the presence of TMA (vide infra).

In practice, these values are not very meaningful; in most cases, rapid and exothermic polymerization was observed under these conditions followed by an (equally) rapid decline in the rate of monomer consumption to a much lower steady-state value. Presumably, the latter value is indicative of the actual amount of active catalyst present; the initial phase of these polymerizations can be viewed as a competition reaction for [Zr*] between monomer (which leads to polymerization) and adventitious quenching by, e.g., H_2O.

The interpretation of these results are complicated by the instability of the ion pairs derived from **3** and **1a** (and presumably **1b**) at room temperature in toluene solution (vide supra). Under the conditions studied (precontacting in toluene), one would have expected maximal decomposition of the ion pairs into the final products, as outlined previously, and thus the observed catalytic activity and polymer properties could have resulted from any of the species formed. As unimodal molecular weight distributions (MWDs) with M_w/M_n = 2−4 were observed in all cases, one can at least conclude that there is either a single active species present and/or (less likely) the ratio of chain propagation to chain transfer is similar for the different species present.

With a view to overcoming the thermal instability problem, a second procedure was developed for screening these materials and the results are summarized in Table 3. Instead of premixing the catalyst and cocatalyst, the requisite cocatalyst was introduced first, followed by metallocene **3**. Although this sometimes led to measurable induction periods prior to monomer uptake, this procedure led to much more reproducible results (i.e., temperature control to better than ±2 °C with stable flow profiles) than the protocol involving premixing of the two catalyst components. The second procedure also involved the use of TMA as a scrubbing agent, and the optimal level for this additive was found to be 30 μM (i.e., 90 μM based on Al−Me bonds) using the catalyst combination **3**/$B(C_6F_5)_3$ (each at ca. 15 μM); lower TMA loadings resulted in low/no ethylene consumption, while higher loadings also suppressed activity (to a lesser extent), possibly via formation of [$Cp_2Zr(\mu$-$Me)_2AlMe_2$][X] complexes in situ.[26]

From the activity data summarized in Table 3, it is clear that the most active cocatalyst is $B(C_6F_5)_3$. With this cocatalyst, the mode of catalyst formation, i.e., premixed vs in situ generation, has no effect on polymerization activity (entries 1 vs 2). In entry 3, no TMA was used as a scrubbing agent and 60 μM **3** was initially present but *only* 15 μM $B(C_6F_5)_3$ was introduced; the fact that the productivity was comparable to the polymerizations conducted in the presence of TMA indicates that, at the levels used, this additive has little effect on either polymerization activity or polymer properties.

Cocatalysts **1a** and **1b** were closely equivalent and gave rise to catalysts which were about 50−60% less active than **3**/$B(C_6F_5)_3$ under equivalent conditions (Table 3, entries 4 and 6 vs 1). The MW of the PE produced was somewhat higher in the case of **1a** compared to **1b** or $B(C_6F_5)_3$, although one should be cautious in concluding that the MWs are significantly different given the uncertainties in both MW determination and polymerization conditions. Interestingly, the MWD of the polymers produced using either **1a** or **1b** were significantly narrower than those using $B(C_6F_5)_3$. This is quite surprising given the thermal instability of the ion pairs derived from **3** or **1a** (vide supra).

Given the uncertainty as to which species was producing polymer in polymerizations involving **1a** or **1b**, ethylene polymerizations were also conducted with the *initially* formed decomposition products from **3** and **1a** (i.e., **4a** and $MeB(C_6F_5)_2$, **7**). The polymerization of ethylene was first examined with zirconacyclopropene **4a** or with a mixture of **1a** and **4a** (1:1 mol ratio). The lack of measurable ethylene uptake during these experiments indicates that complex **4a** is inactive in ethylene polymerization, despite the fact that this complex does react with ethylene at room temperature.[27]

In contrast, polymerization studies involving the use of $MeB(C_6F_5)_2$ as a cocatalyst with **3** produced high molecular weight polyethylene with a narrow MWD (Table 3, entry 9). The catalytic activity was somewhat lower than that observed for **1a** or **1b**, but the MW and MWD were comparable to those observed when using either cocatalyst **1a** or **1b**. These results suggest that the polymerization observed in the presence of diboranes **1** can be interpreted as arising from $MeB(C_6F_5)_2$ and **3**.

(25) Catalysts were introduced into the reactor by using a sample bomb and blowing the contents of this into the reactor using N_2. The precontacting time reflects the amount of time needed to fill the bomb in the glovebox followed by removal and attachment to the reactor system.

(26) Bochmann, M.; Lancaster, S. *Angew. Chem., Int. Ed. Engl.* **1994**, *33*, 1634.

(27) Complex **4a** reacts with 1 equiv of ethylene to form a compound of unknown structure: Köhler, K.; Piers, W. E. Unpublished results.

Table 4. Kinetics of Ethylene Polymerization Using Cp_2ZrMe_2 (3) and Boron Cocatalysts

entry	conditions[a]	cocatalyst	R_p[b]	k_p[Zr*][c]	X_n (K)	R_{tr}[d]
1	1	$B(C_6F_5)_3$	5.9(0.6)	8.2(0.8)	7.0(0.2)	8.4(1.1)
2	4	**1a**	2.0(0.2)	2.8(0.3)	9.6(0.9)	2.1(0.4)
3	6	**1b**	2.4(0.2)	3.3(0.3)	7.3(0.4)	3.3(0.4)
4	9	**7**	2.4(0.2)	3.3(0.3)	8.7(0.5)	2.7(0.4)

[a] For polymerization conditions, see the appropriate entries in Table 2. [b] Rate of polymerization in 10^{-4} M s^{-1} as measured by calibrated mass flow meters at steady state. [c] Value (10^{-4} s^{-1}) obtained by dividing R_p by $[C_2H_4]$ at the temperature indicated. Ethylene solubility in toluene at various temperatures and 75 psi was estimated using methods described in Wilhelm, E.; Battino, R. *Chem. Rev.* **1973**, *73*, 1. [d] Value calculated from R_p and X_n in 10^{-8} M s^{-1}.

With this in mind, it is instructive to compare the data in Table 3 on a different basis, namely, the steady-state rate of polymerization, coupled with differences in MW. Activity values represent the area under the curve of monomer consumption vs time and thus are not really indicative of instrinsic differences in the rate of polymerization and/or catalyst stability. Qualitatively, catalysts derived from either **1a**, **1b**, or $MeB(C_6F_5)_2$ and **3** were less stable under the polymerization conditions, as revealed by a decline in polymerization rates from peak values, whereas the combination **3**/$B(C_6F_5)_3$ appeared to be more stable (little or no decline from peak values).

Summarized in Table 4 are the steady-state rates of polymerization for the different cocatalysts, as well as an estimate for k_p[Zr*] at steady state (assuming first-order kinetics in monomer concentration) at 30 °C. At this temperature, catalyst decay was minimal using the different cocatalysts and so the results can be meaningfully compared. In addition, we have included estimates for R_{tr}, the rate of chain transfer, based on the number average degree of polymerization observed under the different conditions. [28]

As can be seen from the results summarized in Table 4, within experimental error, the R_p and R_{tr} for **1a**, **1b**, and $MeB(C_6F_5)_2$ are closely comparable while those for **3**/$B(C_6F_5)_3$ are significantly different. Also, the magnitude of R_{tr} is significantly higher (ca. 3 times) for **3**/$B(C_6F_5)_3$ compared to the other catalysts, but the differences in R_p are also of a similar magnitude (ca. 2.5 times). This accounts for the fortuitous formation of PE with similar MW. It is possible that weaker counterion interactions in the former case lead to more facile chain transfer reactions.[2]

The derived values for k_p[Zr*] in Table 4 obviously correlate strongly with R_p. If k_p is characteristic of only the cationic alkyl (i.e., $[Cp_2ZrMe]$), one interpretation of counterion effects is that more strongly coordinating counterions serve to reduce the steady-state concentration of actively growing chains but otherwise do not fundamentally alter the intrinsic reactivity of the cationic alkyl. It might be instructive to determine active site concentrations with simple systems such as these.[29]

The only unexplained phenomenon is the narrower MWD observed in the case of cocatalysts **1a**, **1b**, and $MeB(C_6F_5)_2$ compared to **3**/$B(C_6F_5)_3$. We cannot account for this difference on the basis of the experiments reported here, but it may reflect stabilization of the metal center, by strong counterion association, toward (irreversible) catalyst deactivation in the presence of monomer.

Conclusions. A series of 1,1-di[bis(perfluorophenyl)-boryl]alkenes were prepared and shown to be less prone to loss of $HB(C_6F_5)_2$ than their fully saturated counterparts. Although Lewis acidic enough to activate the simple metallocene **3**, the borate anion formed was unstable at ambient temperatures and decomposed to form a well-defined product mixture. The spectroscopic data obtained on this process suggested that only one of the borane centers is involved in this chemistry, and the structural data on the diboranes themselves provides a plausible explanation as to why this is the case. These observations imply that a wider bite angle (or a > 1 atom linker) is desirable for multidentate Lewis-acid activators. Nonetheless, the diboranes **1a** and **1b** do serve as cocatalysts for the polymerization of ethylene using Cp_2ZrMe_2. On the basis of these data, as well as that involving reactions of **1a** and **1b** with **3**, it seems probable that the active species in both cases is $[Cp_2ZrMe]^+[Me_2B(C_6F_5)_2]^-$, generated in situ from the reaction of $MeB(C_6F_5)_2$ with **3**.

Experimental Section

General. All manipulations of air- and moisture-sensitive materials were undertaken using standard vacuum and Schlenk techniques[30] or in a glovebox under an atmosphere of nitrogen. All solvents were dried and purified by passing through suitable drying agents (alumina and Q5).[31] NMR spectra were recorded in C_6D_6 at room temperature or in C_7D_8 for low-temperature experiments. Data are given in ppm relative to solvent signals for ^1H and ^{13}C spectra or relative to external standards for ^{11}B ($BF_3{\cdot}OEt_2$, 0.0 ppm) and ^{19}F ($CFCl_3$ at 0.0 ppm) experiments. IR data is reported in wavenumbers (cm^{-1}). Elemental analyses were performed by Mrs. Dorothy Fox in the microanalytical laboratory of the Department of Chemistry at the University of Calgary. The complexes $Me_2Sn(C{\equiv}CR)_2$ (R = Bu^t, Ph),[32] Cp_2ZrMe_2,[33] $[Cp_2Zr(H)CH_3]$,[34] $ClB(C_6F_5)_2$,[35] $HB(C_6F_5)_2$,[12] and $MeB(C_6F_5)_2$[36] were prepared using literature methods. $B(C_6F_5)_3$ was purchased from Boulder Scientific, dried by treatment with Me_3SiCl, and sublimed prior to use.

Preparation of $Bu^tC{\equiv}CB(C_6F_5)_2$, 2a. Hexane (20 mL) was condensed into an evacuated flask containing $ClB(C_6F_5)_2$

(28) All of these polymerizations were conducted for time periods between 20 and 30 min following establishment of steady-state conditions (i.e., constant mass flow vs time). On the basis of the turnover numbers calculated from R_p in Table 4 (assuming all of the added Cp_2ZrMe_2 is active) and the degree of polymerization, 2−3 polymer chains were produced per Zr atom over this time period using cocatalysts **1a**, **1b**, or $MeB(C_6F_5)_2$. Thus, the calculated values of R_{tr} represent true chain-transfer rates as opposed to rates of termination; the lack of significant decline in R_p over this time period at 30 °C also indicates catalyst stability under these conditions. Evidently, the presence of monomer (or a growing polymer chain) hinders the aryl transfer reaction observed when Cp_2ZrMe_2 and $MeB(C_6F_5)_2$ are mixed at room temperature.

(29) (a) Marques, M. M.; Tait, P. J. T.; Mejzlík, J.; Dias, A. R. *J. Polym. Sci., Part A.* **1998**, *36*, 573. (b) Tait, P. J. T. In Transition Metal Catalyzed Polymerization: Alkenes and Dienes; Quirk, R. P., Ed.; Hartwood Acadademic Publishers: New York, 1983; p 115.

(30) Shriver, D. F.; Drezdzon, M. A. The Manipulation of Air-Sensitive Compounds, 2nd ed.; Wiley: New York, 1986.

(31) Pangborn, A. B.; Giardello, M. A.; Grubbs, R. H.; Rosen, R. K.; Timmers, F. J. *Organometallics* **1996**, *15*, 1518.

(32) Wrackmeyer, B.; Kundler, S.; Boese, R. *Chem. Ber.* **1993**, *126*, 1361.

(33) Samuel, E.; Rausch, M. D. *J. Am. Chem. Soc.* **1973**, *95*, 6263.

(34) (a) Jordan, R. F.; Bajgur, C. S.; Dasher, W. E.; Rheingold, A. L. *Organometallics* **1987**, *6*, 1041. (b) Gell, K. I.; Posin, B.; Schwartz, J.; Williams, G. M. *J. Am. Chem. Soc.* **1982**, *104*, 1846.

(35) Chambers, R. D.; Chivers, T. *J. Chem. Soc.* **1965**, 3933.

(36) Biagini, P.; Lugli, G.; Garbassi, F.; Andreussi, P. Eur. Pat. Appl. EP 667,357, 1995.

(245 mg, 0.643 mmol) at −78 °C, and $Me_2Sn(C{\equiv}CBu^t)_2$ (100 mg, 0.322 mmol) dissolved in hexane (10 mL) was added dropwise. After the reaction solution was stirred for 1 h at −78 °C, it was warmed to 25 °C and stirred for a further hour. The hexane was removed, and the Me_2SnCl_2 was separated by sublimation under full vacuum at 30 °C. The residue was recrystallized at −30 °C in benzene/hexane (1:10) and yielded $Bu^tC{\equiv}CB(C_6F_5)_2$ (230 mg, 85%). ^{1}H NMR: δ 1.19 (s, 9H, CCH_3). ^{13}C{^{1}H} NMR: δ 30.4 (*C*CH_3), 30.2 (C*C*H_3). ^{11}B NMR: δ 48.5. ^{19}F NMR: δ −129.1 (m, 4F, *o*-F), −146.5 (m, 2 F, *p*-F), −161.8 (m, 4F, *m*-F). MS: 426 (25) $[M]^+$; 411(70) $[M - Me]^+$. Anal. Calcd for $C_{18}H_9BF_{10}$: C, 50.74; H, 2.13. Found: C, 50.29; H, 2.09.

Preparation of $Bu^t(H)C{=}C[B(C_6F_5)_2]_2$, 1a. Hexane (20 mL) was condensed into an evacuated flask containing $ClB(C_6F_5)_2$ (122 mg, 0.322 mmol) at −78 °C, and $Me_2Sn(C{\equiv}CBu^t)_2$ (50 mg, 0.161 mmol) dissolved in hexane (10 mL) was added. After the reaction solution was stirred for 1 h at −78 °C it was warmed to 25 °C and stirred for a further hour. A clear, colorless solution was formed. $HB(C_6F_5)_2$ (111 mg, 0.322 mmol) was added, which was completely dissolved after 5 min. The hexane was removed, and the Me_2SnCl_2 was separated by sublimation under full vacuum at 25 °C. The residue was recrystallized at −30 °C in benzene/hexane (1:10) and yielded $Bu^t(H)C{=}C[B(C_6F_5)_2]_2$ (220 mg, 90%). ^{1}H NMR: δ 7.16 (s, 1H, *H*C=), 0.87 (s, 9H CCH_3). ^{13}C{^{1}H} NMR: δ 183.6 (H*C*=), 39.0 (*C*CH_3), 29.2 (C*C*H_3). ^{11}B NMR: δ 39.9. ^{19}F NMR: δ −126.5 (m, 4F, *o*-F), −130.1 (m, 4F, *o*-F), −143.3 (m, 2 F, *p*-F), −148.7 (t, 2 F, *p*-F), −160.5 (m, 4F, *m*-F), −160.6 (m, 4F, *m*-F). IR (KBr pellet): 2972 (w), 1649 (m), 1644 (m), 1550 (m), 1524 (m), 1478 (s), 1391 (m), 1312 (m), 1210 (m), 1178 (m), 975 (s). EI-MS: 772 (40) $[M^+]$, 604 (80) $[M - C_6F_5]^+$, 346 (30) $[HB(C_6F_5)_2]^+$, 258 (50) $[M - HB(C_6F_5)_2 - C_6F_5]^+$, 57 (80) $[Bu^t]^+$. Anal. Calcd for $C_{30}H_{10}B_2F_{20}$: C, 46.67; H, 1.31. Found: C, 46.47; H, 0.81.

Preparation of $PhC{\equiv}CB(C_6F_5)_2$, 2b. Hexane (20 mL) was condensed into an evacuated flask containing $ClB(C_6F_5)_2$ (217 mg, 0.570 mmol) at −78 °C, and $Me_2Sn(C{\equiv}CPh)_2$ (100 mg, 0.285 mmol) dissolved in hexane (10 mL) was added. After the reaction solution was stirred for 1 h at −78 °C, it was warmed to 25 °C and stirred for a further hour. A clear, light yellow solution was observed. The hexane was removed, and the Me_2SnCl_2 was separated by sublimation under full vacuum at 25 °C. The residue was recrystallized at −30 °C in benzene/hexane (1:10) and yielded $PhC{\equiv}CB(C_6F_5)_2$ (190 mg, 75%). ^{1}H NMR: δ 7.55 (m, 2H, C_6H_5), 6.95 (m, 3H, C_6H_5). ^{13}C{^{1}H} NMR: δ 134.3, 132.3, 129.4, 122.2 (C_6H_5). ^{11}B NMR: δ 47.4. ^{19}F NMR: δ −128.5 (m, 4F, *o*-F), −145.9 (m, 2F, *p*-F), −161.5 (m, 4F, *m*-F). MS: 446 (90) $[M]^+$. Anal. Calcd for $C_{20}H_5BF_{10}$: C, 53.85; H, 1.13. Found: C, 53.63; H, 0.76.

Preparation of $Ph(H)C{=}C[B(C_6F_5)_2]_2$, 1b. Hexane (20 mL) was condensed into an evacuated flask containing $ClB(C_6F_5)_2$ (108 mg, 0.285 mmol) at −78 °C, and $Me_2Sn(C{\equiv}CPh)_2$ (50 mg, 0.142 mmol) dissolved in hexane (10 mL) was added. After the reaction solution was stirred for 1 h at −78 °C, it was warmed to 25 °C and stirred for a further hour. A clear, light yellow solution was formed. $[HB(C_6F_5)_2]_2$ (99 mg, 0.285 mmol) was added, which was completely dissolved after 5 min. The hexane was removed, and the Me_2SnCl_2 was separated by sublimation under full vacuum at 25 °C. The residue was recrystallized at −30 °C in benzene/hexane (1:10) and yielded $Ph(H)C{=}C[B(C_6F_5)_2]_2$ (180 mg, 80%). ^{1}H NMR: δ 8.27 (s, 1H, *H*C=), 6.95 (m, 2H, C_6H_5), 6.81 (m, 3H, C_6H_5). ^{13}C{^{1}H} NMR: δ 173.1 (H*C*=), 138.6 (C_{ipso}), 133.1, 131.3, 129.2 (C_6H_5). ^{11}B NMR: δ 62.7. ^{19}F NMR: δ −127.2 (d, 4F, *o*-F), −129.8 (m, 4F, *o*-F), −144.4 (m, 2F, *p*-F), −147.9 (t, 2F, *p*-F), −160.3 (m, 4F, *m*-F), −161.1 (m, 4F, *m*-F). IR (KBr pellet): 1649 (m), 1644 (m), 1519 (s), 1481 (vs), 1389 (m), 1310 (m), 1202 (m), 1150 (m), 975 (s). EI-MS: 791 (50) $[M]^+$, 77 (100) $[C_6H_5]^+$. Anal. Calcd for $C_{32}H_6B_2F_{20}$: C, 48.53; H, 0.53. Found: C, 48.07; H, 0.26.

Preparation of $Me_2Sn(C{\equiv}CC_6F_5)_2$. Ether (20 mL) was condensed into an evacuated flask, and $HC{\equiv}CC_6F_5$ (200 mg, 1.04 mmol) was added at −78 °C. After addition of BuLi/hexane (0.65 mL, 1.04 mmol, 1.6M) at −78 °C, it was warmed to 25 °C and stirred for 30 min. Me_2SnCl_2 (114 mg, 0.52 mmol) was added in one portion, and the mixture was stirred overnight. A white precipitate was formed. The ether was removed in vacuo, and the residue was dissolved in hexane (20 mL). After filtration, the solvent was removed in vacuo, yielding a colorless powder. Crystallization at −30 °C in hexane yielded $Me_2Sn(C{\equiv}CC_6F_5)_2$ (166 mg, 60%). ^{1}H NMR: δ 0.20 (s, 6H, SnCH_3). ^{13}C{^{1}H} NMR: δ 148.3 (m, C_6F_5), 142.1 (m, C_6F_5), 138.0 (m, C_6F_5), 106.0 (m, SnC≡*C*), 92.7 (m, Sn*C*≡C), −6.2 (s, Sn*C*H_3). ^{19}F NMR: δ −137.0 (m, 4F, *o*-F), −152.4 (m, 2F, *p*-F), −162.0 (m, 4F, *m*-F). IR (KBr pellet): 2155 (w), 1500 (s), 996 (s), 967 (s), 789 (m). EI-MS: $M^+ - Me - 3F$ [460 (20)], $M^+ - Me - C_6F_5$ [348 (10)], $C_2C_6F_5^+$ [192 (80)].

Preparation of $C_6F_5(H)C{=}C[B(C_6F_5)_2]_2$, 1c. Hexane (20 mL) was condensed into an evacuated flask containing $ClB(C_6F_5)_2$ (103 mg, 0.271 mmol) at −78 °C, and $Me_2Sn(C{\equiv}CC_6F_5)_2$ (72 mg, 0.136 mmol) dissolved in hexane (10 mL) was added. After the reaction solution was stirred for 1 h at −78 °C, it was warmed to 25 °C and stirred for a further hour. A yellow, clear solution was formed. $[HB(C_6F_5)_2]_2$ (94 mg, 0.271 mmol) was added, which was completely dissolved after 5 min. The hexane was removed, and the Me_2SnCl_2 was separated by sublimation under full vacuum at 25 °C. The residue was recrystallized at −30 °C in benzene/hexane (1:10) and yielded $C_6F_5(H)C{=}C[B(C_6F_5)_2]_2$ (155 mg, 65%). ^{1}H NMR: δ 7.87 (s, 1H, *H*C=). ^{13}C{^{1}H} NMR: δ 148.8 (H*C*=). ^{11}B NMR: δ 61.8. ^{19}F NMR: δ −126.3 (d, 4F, *o*-F), −128.9 (d, 4F, *o*-F), −141.5 (d, 2F, *o*-F), −142.5 (m, 2F, *p*-F), −145.3 (m, 2F, *p*-F), −146.1 (t, 1F, *p*-F), −158.8 (m, 4F, *m*-F), −159.9 (m, 2F, *m*-F), −160.2 (m, 4F, *m*-F). IR (KBr pellet): 1650 (m), 1644 (m), 1524 (s), 1477 (vs), 1388 (m), 1315 (m), 1165 (m), 975 (s). EI-MS: 882 $[M]^+$. Anal. Calcd for $C_{32}HB_2F_{25}$: C, 43.58; H, 0.11. Found: C, 43.06; H, 0.00.

Reaction of Cp_2ZrMe_2 with 1a (2:1). A sealable 5 mm NMR tube was loaded with Cp_2ZrMe_2 (22 mg, 0.087 mmol) and dissolved in toluene-d_8 (ca. 0.3 mL). The tube was attached to a vacuum line and cooled to −78 °C. A solution of **1a** (33 mg, 0.043 mmol) in d_8-toluene (ca. 0.4 mL) was added by syringe and the tube was flame sealed. The tube was briefly shaken and loaded into a precooled NMR probe (−80 °C) tuned to either ^{1}H or ^{19}F. The ensuing reaction was monitored spectroscopically as a function of temperature. Data for **5a** (−60 °C). ^{1}H NMR: δ 5.62 (s, 20H, C_5H_5), 6.31 (s, 1H, *H*C=), 1.12 (s, 9H, CCH_3), −0.10 (s, 6H, ZrCH_3), −0.39 (s, br, 3H, BCH_3), −1.23 (s, 3 H, ZrCH_3Zr). ^{19}F NMR: δ −123.0 (ABq, br, 1F, J = 113 Hz), −123.2 (ABq, br, 1F, J = 113 Hz), −126.0 (s, br, 1F), −126.3 (s, br, 1F), −126.9 (s, br, 1F), −130.9 (s, br, 1F), −132.7 (s, br, 1F), −138.7 (s, br, 1F), −145.1 (s, br, 1F), −149.9 (s, br, 1F), −157.3 (s, br, 1F), −159.9 (s, br, 1F), −160.4 (s, br, 1F), −161.2 (s, br, 1F), −161.5 (s, br, 1F), −162.2 (s, br, 1F), −163.0 (s, br, 1F), −163.8 (s, br, 2F), −167.2 (s, br, 1F). Data for $Cp_2ZrMeC_6F_5$. ^{1}H NMR: δ 5.63 (s, 10H, C_5H_5), 0.25 (t, 3H, $^5J_{HF}$ = 3.9 Hz, ZrCH_3). ^{13}C NMR: δ 111.4 (C_5H_5), 45.7 (Zr*C*H_3). ^{19}F NMR: δ −115.2 (m, 2 F, o-F), −156.6 (t, 1 F, p-F), −162.2 (m, 2 F, m-F). Data for $Me_2BC_6F_5$. ^{1}H NMR: δ 1.0 (s, br). ^{19}F NMR: δ −130.9 (m, 2 F, o-F), −151.4 (t, 1 F, p-F), −162.6 (m, 2 F, m-F). ^{11}B NMR: δ 80.2.

Reaction of Cp_2ZrMe_2 with 1a (1:1). The same procedure as that described above was employed, using 11 mg (0.43 mmol) of Cp_2ZrMe_2 and 33 mg (0.043 mmol) of **1a**. ^{1}H NMR data for **6a**: 5.30 (s, 10H, C_5H_5), 6.11 (s, 1H, *H*C=), 1.03 (s, 9H, CCH_3), 0.26 (s, 3H, ZrCH_3), −0.39 (s, br, 3H, BCH_3).

Preparation of $Cp_2Zr[Bu^tC{\equiv}CB(C_6F_5)_2]$, 4a. $[Cp_2Zr(H)CH_3]_n$ (92 mg, 0.194 mmol) and $Bu^tC{\equiv}CB(C_6F_5)_2$ (165 mg, 0.387 mmol) were dissolved in toluene (20 mL) at −78 °C. After the reaction solution was stirred for 1 h at −78 °C, it was warmed to 25 °C. A deep red-brown solution was obtained.

Table 5. Summary of Data Collection and Structure Refinement Details for 1a−c

	1a	1b	1c
formula	$C_{30}H_{10}B_2F_{20}$	$C_{32}H_6B_2F_{20}$	$C_{32}HB_2F_{25}$
fw	772.00	791.99	881.95
temp, K	296(2)	160(2)	160(2)
cryst syst	monoclinic	monoclinic	monoclinic
a, Å	17.8248(5)	13.5310(6)	17.318(3)
b, Å	9.0087(5)	14.0523(6)	8.7958(15)
c, Å	19.338(1)	16.1446(7)	21.475(3)
β, °	99.238(2)	102.835(2)	109.633(4)
V, Å^3	3065.0(2)	2993.1(2)	3081.0(9)
space group	$P2_1/c$	$P2_1/n$	$P2_1/c$
Z	4	4	4
d_{calc}, mg m^{-3}	1.673	1.758	1.901
μ, mm^{-1}	0.182	0.189	0.217
cryst size, mm	0.40 × 0.30 × 0.30	0.50 × 0.40 × 0.35	0.18 × 0.16 × 0.12
no. of rflns measd	10 717	23 300	14 929
no. of unique rflns	3907	7135	5410
R_{int}	0.0482	0.0196	0.0785
no. of variables	422	512	537
max, min e density Å^3	0.385/−0.238	0.317/−0.290	0.294/−0.298
R1[a]	0.0746	0.0377	0.0575
wR2[a]	0.1763	0.0978	0.1356
gof	1.089	1.031	0.988

[a] R1 is a conventional *R* factor based on *F* values of reflections having $F^2 > 2\sigma F^2$; wR2 is a weighted *R* factor based on F^2 values of all unique data.

After filtration, the toluene was removed and the residue washed twice with hexane and vacuum-dried yielding a red-brown solid of $Cp_2Zr[Bu^tC{\equiv}CB(C_6F_5)_2]$ (180 mg, 72%). ^{1}H NMR: *δ* 5.62 (s, 10H, C_5H_5), 1.16 (s, 9H, CCH_3). $^{13}C\{^1H\}$ NMR: *δ* 111.2 (C_5H_5), 40.9 (CCH_3), 32.7 (CCH_3). ^{11}B NMR: *δ* 21.5. ^{19}F NMR: *δ* −145.6 (s, br, 4F, *o*-F), −154.8 (t, 2F, *p*-F), −161.6 (m, 4F, *m*-F). EI-MS: 647 (100) $[M]^+$; 590 (20) $[M - Bu^t]^+$, 220 (55), $[Cp_2Zr]^+$, 57 (45) $[Bu^t]^+$. Anal. Calcd for $C_{28}H_{19}BF_{10}Zr$: C, 51.94; H, 2.96. Found: C, 51.50; H, 2.71.

X-ray Crystallography. Measurements were made on a Bruker AXS SMART CCD area-detector diffractometer using graphite-monochromated Mo Kα radiation (λ = 0.710 73 Å). The structures were solved by direct methods and refined on F^2 values by full-matrix least-squares for all unique data. Table 5 gives further details. Programs used were standard Bruker SMART (control) and SAINT (integration); SHELXTL[37] for structure solution, refinement, and molecular graphics; and local programs.

Ethylene Polymerizations. Polymerizations were performed in a 1 L Autoclave Engineers Zipperclave stainless steel reactor equipped with an overhead stirrer and a spiral-wound external cooling jacket. All polymerizations were conducted at a stirring rate of 1000 rpm. A Neslab RTE-110 refrigerating circulator passed a coolant mixture (ethylene glycol/water) through the reactor jacket. An RTD-220 temperature controller (Neslab) controlled the temperature (±1 °C), while a remote sensor (Neslab RS2) monitored the reaction solution at the temperature and cycled the circulator heater on or off as required. The flow of monomer into the reactor (to maintain a given head pressure) was measured using a mass flow meter and a mass flow controller (Matheson Multiple Dynablender-8219). The progress of polymerizations was monitored (monomer flow rate(s) and internal temperature) using an IBM PC with a data acquisition card and associated software.

Procedure 1: Premixing of Catalyst and Cocatalyst. Toluene (500 mL) was presaturated with monomer at the specified temperature and pressure (75 psi). A 25 mL amount of a toluene solution of **3** and cocatalyst (ratio 1:1.2) was prepared in a glovebox and transferred to a 50 mL stainless steel sample vessel. Polymerizations were initiated by injection of the solution into the reactor using a slight overpressure of N_2 (ca. 5 psi). Polymerizations were terminated by venting the monomer and rapidly draining the polymer solution into a small volume of methanol. The polyethylene was filtered, washed with methanol, and dried in a vacuum oven for 24 h at 80 °C.

Procedure 2: In Situ Catalyst Generation. A toluene solution (25 mL) of $AlMe_3$ and cocatalyst was transferred into the reactor, containing toluene (450 mL), using a 50 mL sample vessel. The solution was allowed to stir for at least 30 min at the desired process temperature while saturating with monomer. Polymerizations were initiated by injection of a solution of **3** in toluene (25 mL) into the reactor using an overpressurized sample cylinder. Polymerizations were terminated by venting the monomer and rapidly draining the polymer solution into a small volume of methanol. The polyethylene was filtered, washed with methanol, and dried in a vacuum oven for 24 h at 80 °C.

Polymer Characterization. Polymer molecular weights and distributions were determined by gel-permeation chromatography (GPC) using a Water 150C chromatograph on a Jordi mixed-bed column (10−10^3 Å) employing a differential refractive index detector at 145 °C in 1,2,4-TCB solution. Sample dissolution (0.1% w/v) was accomplished by rotating the samples in an oven operating at 160 °C for a few hours with 0.1% BHT as the antioxidant. Samples were eluted at a flow rate of 1.0 mL/min, and columns were calibrated using both a broad MWD PE and narrow MWD PS standards.

Acknowledgment. Funding for this work from the Natural Sciences and Engineering Research Council of Canada Strategic Project Grant and Novachem Ltd. of Calgary, Alberta, Canada, is gratefully acknowledged. W.C. acknowledges funding from the Engineering and Physical Sciences Research Council, U.K. W.E.P. also thanks the Alfred P. Sloan Foundation for a Research Fellowship (1996−2000). K.K. acknowledges the DFG for a Postdoctoral Fellowship.

Supporting Information Available: Full tables of crystallographic data, atomic parameters, hydrogen parameters, atomic coordinates, anisotropic thermal parameters, and complete bond distances and angles for **1a−c** (26 pages). Ordering information is given on any current masthead page.

OM980259E

(37) Sheldrick, G. M. *SHELXTL*, version 5; Bruker AXS Inc.: Madison, WI, 1994.